

Three-dimensional Computational Fluid Dynamics Based Design of Hull and Propeller of an Underwater Vehicle

Rameez Shahab¹, Ahmed Asees Aamir^{1,a}, Dr. Muahmmad SaifUllah Khalid², Dr. Abdul Haq³

¹Department of Mechanical Engineering, CEME (NUST), Rawalpindi.

² Research Center for Fluid Machinery Engineering and Technology, Jiangsu University, Zhenjiang, China.

³ Centre of Excellence in Science and Applied Technologies (CESAT), Islamabad, Pakistan.

^aaamirasees@gmail.com

Abstract—Underwater Vehicles are now used widely for mining, marine research, and military surveillance etc. Design of the vehicle is of paramount importance as efficiency of the mechanical equipment is one of the important areas of research these days. A little increase in efficiency can help saving a large amount of fuel, and consequently, decreasing amount of money required to be spent and weight of vehicle. Design study of the vehicle may be carried out by performing a parametric study related to the hydrodynamics of the vehicle. Considering the geometric and kinematic characteristics of the blades and the hull, this study aims to figure out a configuration for greater hydrodynamic efficiency of the vehicle. Since real-time experimental equipment is expensive, we adopted a computational approach. For the present study, simulations for incompressible viscous flow over the underwater vehicle through a finite-volume method based industrial flow solver-ANSYS Fluent were employed. During the simulations, we swept over a parametric space consisting of hull shape, aspect ratio of the vehicle, and Reynold's number.

Keywords— Underwater Vehicle, hydrodynamics, parametric space, Hull, Propeller, CFD

I. INTRODUCTION

Autonomous Underwater Vehicle (AUV) is a robot that travels underwater without taking any input from any operator for doing its required operations. AUV falls under the umbrella of the group unmanned underwater vehicles-a classification that also includes non-autonomous remotely operated underwater vehicles. University of Washington in 1957 developed first AUV, that was a research purpose vehicle and was used to study diffusion, wake patterns of submarines and acoustic transmission [1]. Massachusetts Institute of Technology also developed some AUVs in the 1970s [1]. Simultaneously, Soviet Union also developed AUVs, which remained unnoticed due to political hospitalities. AUVs are used mainly for three purposes: commercial, research and hobby. In commercial usage, AUVs are used to investigate ocean floor to examine its suitability for operations of submarines making it an important tool in military operations. In research, it is also used to study marine life or ocean floors. It can be used to collect data about enemy movements in the sea, or to install sensors at different places so that it can then be used to take real-time data. It can also be used to investigate air-crashes in the sea. Different competitions all over the world like International Autonomous Underwater Vehicle

Competition, Singapore AUV Challenge etc are conducted all over the world.

II. LITERATURE REVIEW

Hayati et al. [2] studied different propellers behind hulls with different parameters like advance ratio to investigate their performance using computational fluid dynamics (CFD) based numerical techniques. It was validated against experimental data already reported in the literature. According to this study, high angle of attack produced more thrust, and consequently required more torque to rotate the propeller. Thrust and torque coefficients in open water conditions were overestimated by at least 8% in the paper. Du et al. [3] carried out research on docking of underwater vehicle. For successful operation of underwater vehicle, docking is essential because it is used to charge batteries and develop communication links that improves efficiency of the operation. For successful docking, its hydrodynamics has to be known precisely. For this purpose, the tools and techniques of CFD were employed. Their simulation results indicated an increase in hydrodynamic coefficients as AUV moves near conical section of docking device. Then AUV enters constant cross-sectional part where moment coefficient shows a rapid increase, and then decreases sharply. Most important result here is the use of open bottom docking device reduces drag coefficient. Papadopoulos et al. [4] studied hydrodynamic forces on an AUV in riverine environment as opposed to normal trend of studying the forces in open ocean water. This type of dynamics includes strong side and head-on currents. These currents also depend upon the topology of the surface around the AUV in the pool. This type of flow is highly turbulent compared to the ocean flow. A simple torpedo and NACA profiled bodies were sought in this paper for riverine flow. Their study also shows drag plot. Toxopeus et al. [5] studied effect of appendages on the AUV used for maneuvering. These appendages enhance friction drag and also deteriorate inflow to aft control surface of the propeller, hence its design is scrutinized and optimized through the use of CFD. The study discussed how formation of better wake be formed, and resistance can be reduced using design of the junction. Their results indicated that resistance and wake quality depends on thickness of the sail. Thick sail produces large resistance, and wake is distorted. A suitable cuff can eliminate the horseshoe vortex, which is a simplified representation of the vortex system of awing. Cuff does not create any problem in maneuverability of the ship. de Sousa et al. [7] worked out with detailed CFD simulation for flow over a

hull shape of an AUV. These investigations are distinguished from the previous studies as it provides a mathematical equation of the geometric profile. The governing mathematical expression to define the geometry of the bow and stern is provided for the AUV. It is shown that it is more efficient than the other shapes. Its drag coefficient is almost equal to an ellipsoid, but with 10.3% more volume of the structure. This drag coefficient is seven times smaller than a cylinder for similar conditions.

III. STUDY OBJECTIVES

The present study reports the conclusions drawn from two dimensional (2D) simulations of different hull shapes, 3D simulations of hull and propellers, and details of the hydrodynamic analysis. 2D simulations were performed on the basic hull shapes for the comparison of drag coefficients (C_d) from current methodology, and those reported in the literature. The objective of 2D study were to determine an optimized hull shape that would cause minimum drag on the AUV. 3D simulations were performed with optimized hull shape and propeller with different number of blades. Another objective of the study was to determine the effect of geometric and kinematic parameters on the performance of the propellers, to visualize the flow and to compute the drag coefficient, coefficient of moment and coefficient of thrust.

IV. NUMERICAL METHODOLOGY

CFD analysis is conducted using a commercial multi-purpose CFD solver-ANSYS CFX and ANSYS Fluent [6]. The code uses Reynolds Averaged Navier-Stokes Equation and the Finite Volume Method to numerically solve the governing equations for the flow. The SpalartAllmaras (SA) turbulence model was used to predict the separation of flow accurately. Although S-A model is used for aerodynamics applications, but Dongyan et al. [8] applied S-A model to blade of canoe in water and compared results with results of other turbulence models, they were in significant agreement. Hence, to save time and looking at robustness of the model, we used S-A model for our simulations.

A. Geometry

Before generating grid and moving further with solution, geometry was imported. For that, files from SolidWorks were saved in the STEP format, and was then imported in ICEM-CFD for further grid generation.

1) 2D Geometry

Two types of hull were used: hemispherical and conical, with different D/L values, where D is the diameter of the frontal section of the hull, and L shows its length.

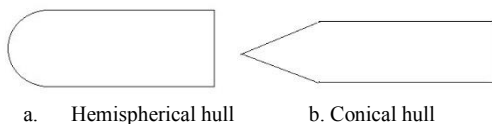


Fig. 1: Hull Shapes

Another hull is commonly found, where the tail is tapered with a conical shape. It helps control vortex shedding, and thus

reducing pressure drag. So, this hull was also included in the study.



Fig. 2: Hull with Tail

2) 3D Geometry

Optimized hull shape from 2D simulations was used with different propellers for 3D simulations. One of the complete geometries imported for meshing is shown below.



Fig. 3: Hull and Propeller

B. Grid Generation

Grid was generated after the geometry was imported. A high quality grid will govern the accuracy of the solution and it will also ensure the quicker convergence for iterative solutions. Y+ value ensures proper size of cells near domain wall for the particular turbulence model used. In this study, unstructured triangular grid is used. Grid is fine near the walls of the hull, and in the wake with coarser element sizes in the far field. Moreover, inflation layers were used to resolve the boundary layer.

1) 2D Grid

Table 1: Properties of 2D Grid

Grid Method	Triangular Grid
Y+ Value	30
Domain Length	35m
No of Inflation Layers	10-15

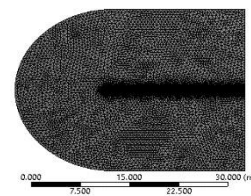


Fig. 4: Grid of 2-D Hemispherical Hull

Using these properties, three different grids were generated. Coarse grid has 30,000, medium grid has 60,000 and fine grid has 100,000 elements.

2) 3D Grid

The properties of three-dimensional (3D) meshing are shown in Table 2 that was used to produce surface and volume grids around the propeller and hull, and then for the complete

body. To generate this grid, a Robust Octree grid technique was utilized. The grid was refined to improve quality of the grid. The volume mesh was created through Delaunay meshing technique from the existing surface grid, so that high quality volume elements could be generated. Prism Layers were used to resolve the boundary layer on the hull and the propeller surfaces. Finally, Laplace smoothing was performed to increase quality of the grid.

Table 2: Properties of 3D Grid

Grid Method	Unstructured Tetrahedral
Prism Layer Height (Propeller)	0.0007
Prism Layer Height (Hull)	0.0003
No of Prism Layers	5-10
No of grid elements	1-2 million



Fig. 5: Surface Grid on Propeller

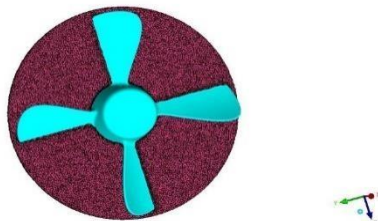


Fig. 6: Volume Grid in rotating domain



Fig. 7: Surface Grid on Hull Surface

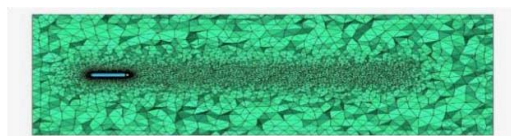


Fig. 8: Volumes Grid in Stationary domain

Fine grid was used near hull and propeller surfaces and in wake and coarse grid was used in far-field.

C. Solver Settings

For 2-D simulations, temporal simulations are done using the Pressure Implicit with Splitting of Operator (PISO) solution method. Reynold's number based on the incoming velocity and length of the geometry used was one thousand, and reference values to compute the hydrodynamic coefficients were taken from the inlet conditions. The time-steps used was 0.004 sec and 0.0004 sec to check the convergence.

For 3-D simulations, two zones were created: a rotating zone around propeller, and a stationary zone in the outer region. Both the zones were meshed separately, and then appended in ANSYS Fluent. Revolutions per minute (RPM) were specified to the rotating zone through the frame motion option in the solver. Pressure-velocity coupling for incompressible Navier-Stokes equations was used. For these simulations, multiple reference frame (MRF) method gave steady state solutions.

D. Turbulence model selection

Turbulence model is used to estimate kinematic eddy turbulent viscosity. For this study, Spalart–Allmaras turbulence model is used which is a one-equation turbulence model, and is considered suitable for most of the aerodynamic and hydrodynamic cases.

E. Boundary Conditions

Boundary conditions are the most important part of CFD analysis. Incorrect boundary conditions will result in incorrect solutions. So it required to specify the correct boundary conditions. Velocity inlet, pressure outlet and hull surface was treated as 'wall'. In 3-D simulations, surface between stationary and rotating zone was treated as interface.

F. Grid Independence

A specific case with the same boundary conditions and geometry was simulated with continuously increasing grid elements and resulting Cd were compared. Grid was increased gradually, until no further significant change in Cd was noticed.

1)2D Grid Convergence

Grid convergence was achieved at approximately 80,000 elements in 2D simulations and in 3D at 0.9 million elements.

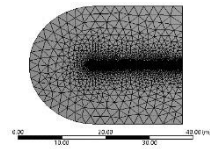


Fig. 9.1: Coarse Grid

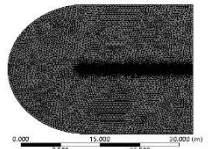


Fig. 9.2: Medium Grid

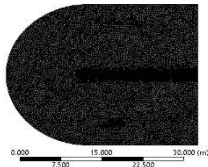


Fig. 9.3: Fine Grid

Table 3: Comparison of Drag Coefficient with Number of Nodes

Number of Nodes	Cd
34,614	0.151
60,584	0.148
102,814	0.148

This comparison showed that the difference between drag coefficients of case 2 and case 3 is negligible. Hence, any one of the both grids may be employed for further simulations. Case 2 had coarser grid as compared to that in case 3, and will converge in less time than without significant loss of accuracy, so grid of case 2 was utilized for further simulation.

2)3D Grid Independence

Six grids were used with number of elements ranging from 0.2 to 1.5 million. Thrust coefficient and coefficient of moment of the propeller were also computed for the grid independence study. The final 3-D grid produced is shown in the figure below:



Fig. 10: Surface Mesh on Hull

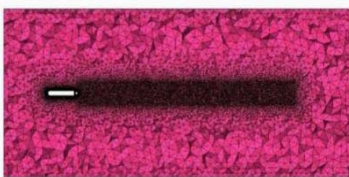


Fig. 11: Volume Grid in Domain

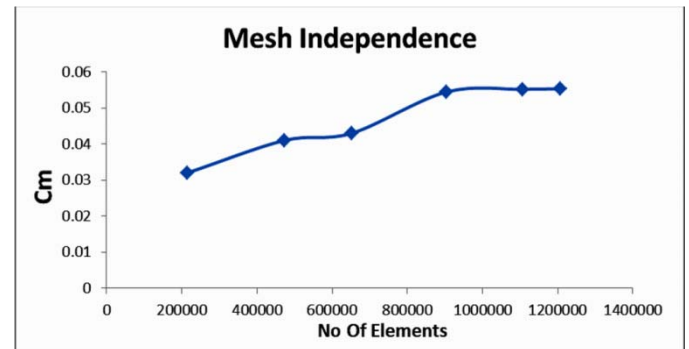


Fig. 12: Plot of Cm (coefficient of moment) vs Grid elements

G. Time Step Convergence

In the study, 2D simulations were transient. So different time steps were used and time step convergence was checked. The solution was considered as independent of grid because there was negligible change in results as shown in table 4.

Table 4: Comparison of Drag Coefficient with Time step size

Time Step Size	Cd
0.004	0.1463
0.002	0.1462
.00004	0.1462

V. VALIDATION

Propeller thrust and torque coefficient were validated by comparison with results reported by Wang et al. [9]. Results agreed reasonably. The details of this comparison is shown in Table 5.

Table 5: Validation of Ct

Advance Ratio, J (V/nD)	Ct (CFD)	Reference Test Results[9]	Percentage Difference
0.4	0.654	0.625	4.43
0.5	0.6	0.61	1.6
0.7	0.52	0.53	1.92
0.8	0.47	0.49	4.26
0.9	0.39	0.41	5.12
1	0.37	0.39	5.40
1.12	0.30	0.31	3.33

Validation of drag of 3-D hull was done by de Sousa et al. [7] as shown in table 6.

Table 6: Results for Validation of the Present Methodology

Inlet velocity (m/sec)	Cd (CFD)	Cd (Reference [7])	Error
2.8	0.122	0.1262	3.32%

VI. RESULTS

A. 2-D Hull

For 2D simulations, two types of hull were considered: triangular and hemispherical. Among those, it was seen that the hemispherical hull gave less drag as compared to the triangular hull. For hemispherical hull, it was observed that as D/L is reduced drag decreased. This is due to the increasing slenderness of the body. Accordingly, it implies that body will present lesser frontal area to disturb the flow, and the associated vortex shedding may be delayed which may result in reduction of the pressure drag. The drag due to skin friction, although not that significant, will also reduce due to decreased surface area. A comparison for Cd computed for both of these shapes is shown here in fig. 13(1-2).

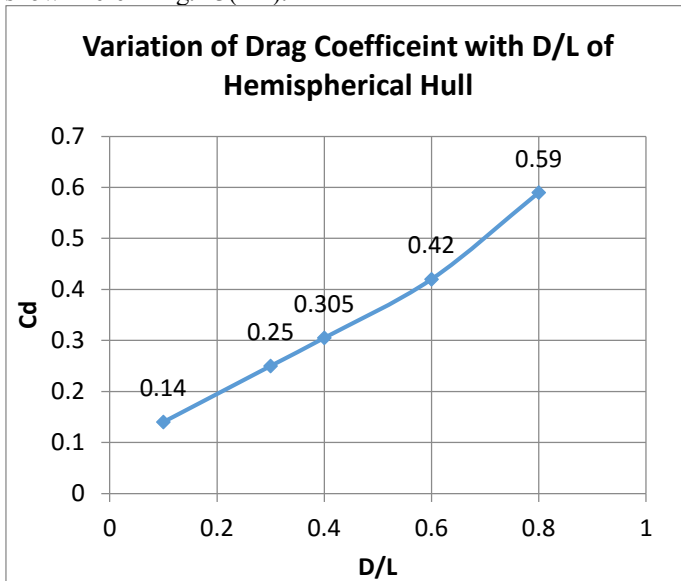


Fig. 13.1: Comparison of Cd against D/L Ratio of Hemispherical Hull

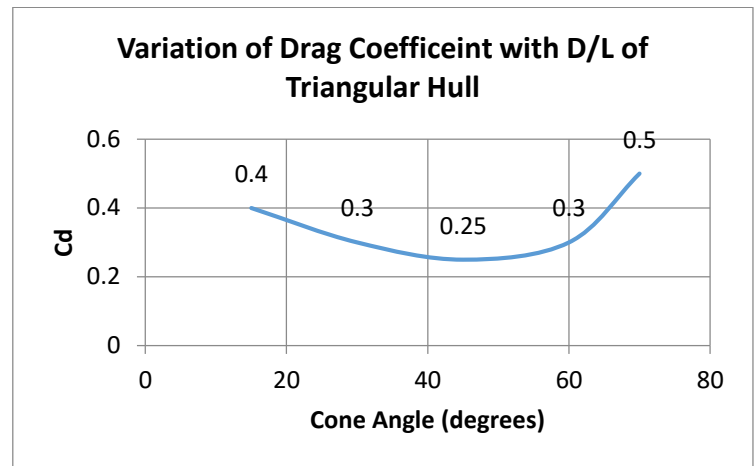


Fig. 13.2: Comparison of Cd against D/L Triangular Ratio

B. 3-D Hull

Simulations on 3-D hull were performed with different oncoming flow velocities. It was observed that Cd of the hull decreased with the inlet velocity. This decrease, however, is negligible. In case of the hull, a particular Cd is valid for a long range of Reynold's Number. A very large change in Reynold's number will be required for a visible change in Cd. It was observed that Cd is almost the same with the inlet velocities taken into account. The trend is shown in the graph below. Through the presented comparison here, the hemispherical hull with D/L=0.1 (Cd=0.15) was selected for 3-D hull study as it experiences the lowest value for Cd; as evident by fig 13.

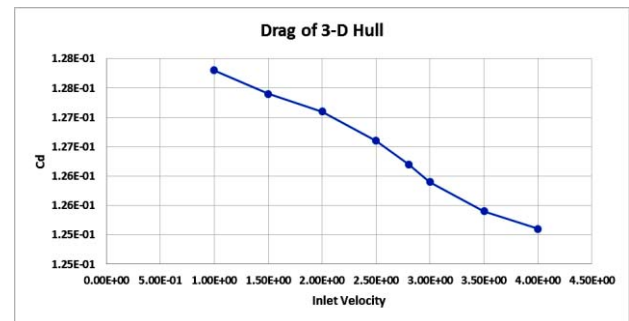


Fig. 14: Cd for different inlet velocities

C. Propeller

There are total three types of propellers that were analyzed in the study

- Three bladed propeller
- Four bladed propeller
- Five bladed propeller

Propellers were analyzed against their advance ratio; J. Advance ratio is defined as ratio of the free-stream velocity to the propeller tip speed. When propeller is in rotation, it will push the fluid behind, and exert force to move in the forward direction. This speed is referred as free stream speed.

Mathematically, J can be defined as,

$$J=V/nD$$

where,

- J is the advance ratio
- V is the free stream velocity
- n is propeller rotational speed in rps
- D is diameter of propeller

Each propeller was analyzed with a range of values for J, and the results are presented here. In case of the propellers, as the advance ratio is increased, velocity must increase. If velocity increases, propeller will present more resistance to the oncoming flow in lesser time, and hence drag will increase. That will in turn decrease C_t (thrust coefficient). Since net thrust is the vector sum of thrust generated by the propeller and drag induced on propeller, and these two quantities are opposite in direction, so they are subtracted from each other. Since velocity increases, drag increase, hence net thrust will decrease.

COMPARISON OF C_t OF DIFFERENT PROPELLERS

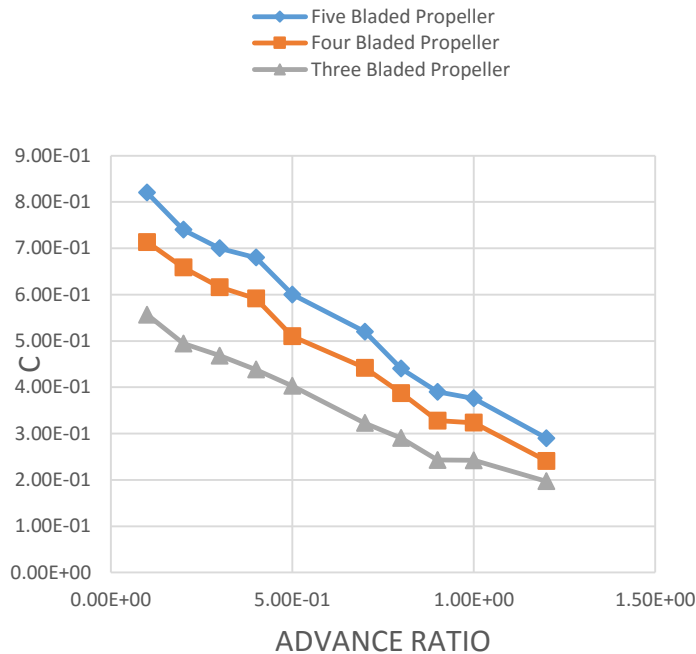


Fig. 15: Comparison of C_t of All Propellers

A comparison of all the propellers was shown above. It presents that in all propellers, the trend by which thrust of propeller diminishes is the same. However, five bladed propeller produces more thrust in absolute terms than the four bladed one, that in turn produces more thrust as compared to the three bladed propeller. The increase in thrust is primarily due to more number of blades. More number of blades produce more thrust by dislocating more amount of water in the flow environment. Next property analyzed is the coefficient of moment. C_m is the product of drag on the propeller and the distance from the center of propeller. This is a measure of torque required by the

propeller to move with a fixed RPM. In our study, it is seen that C_m decreases with the advance ratio. It happened due to the fact that when RPM is decreased, advance ratio will increase (inverse relation) and hence lesser torque will be required for the propeller to move under similar conditions. All the propellers showed the same pattern of decrease in C_m when advance ratio is increased.

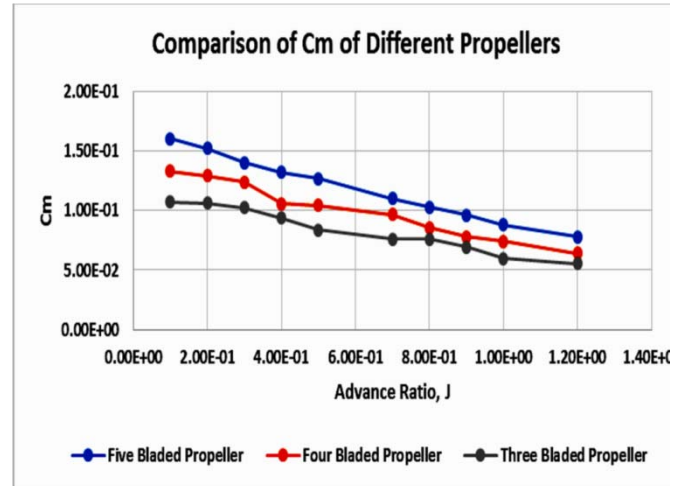


Fig. 16: Comparison of C_m of All Propellers

This concluded our exploration on propeller for the present study. In a nutshell, apart from the absolute values of results it can be inferred from the results that,

- Propellers can be analyzed in terms of advance ratio, J
- C_t decreases as advance ratio increase due to increase in velocity that, in turn, increases pressure drag
- C_m decreases as advance ratio increase due to decrease in RPM and hence lesser moment will be required for propeller to work.

VII.FLOW VISUALIZATION

Flow visualization is an important and powerful tool associated with the use of CFD. It helps enhance our understanding for the working of the system. A plot of velocity contours around 2-D hemispherical hull shown in fig. 17.1. It shows vortex shedding in the wake. These vortices shed periodically and cause an increase in pressure drag. During this investigation, it was observed that vortex shedding increased with an increase in Reynolds number.

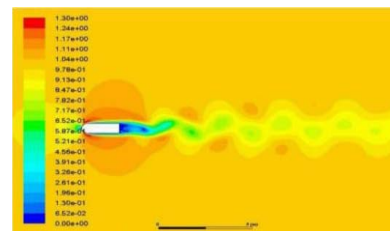


Fig. 17.1: Velocity contours of 2-D Hemispherical Hull at high Reynold's Number

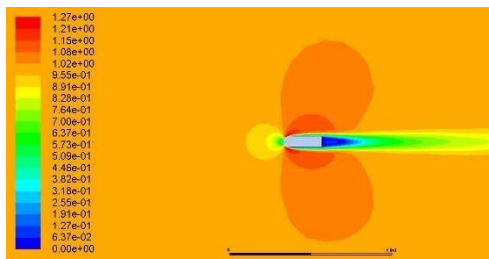


Fig. 17.2: Velocity contours of 2-D hemispherical Hull at Low Reynold's Number

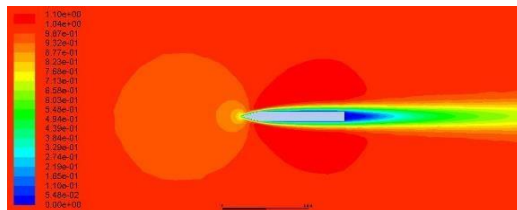


Fig. 18: Velocity Contours of 2-D Triangular Hull

Velocity contours on the surface of 3-D hemispherical hull are shown in fig. 19. Since no-slip condition was applied on the surface of hull, water at the surface of the hull will remain stationary.

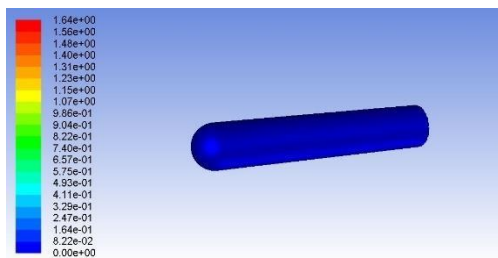


Fig. 19: Velocity contours of 3-D hemispherical hull

Velocity contours were obtained on propeller surface. It shows that the surface velocity increases outwards radially. It is a visualization of no-slip condition. As we move radially outwards, tangential velocity of propeller blade increases, and hence the velocity of water increases.

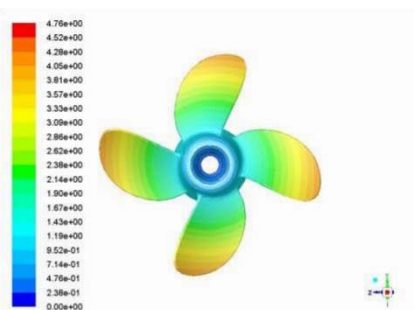


Fig. 20: Velocity Contours on surface of propellers

To have a clear understating of the wake behind the propeller, velocity contours at different distances in the wake were obtained. The trend displays that as we move away from

propeller, flow separation diminished. The pattern is shown in Fig. 21(1-5) below, as distance in the wake from the propeller increases. The distance is minimum in fig 21.1, and largest in in fig 28.5.

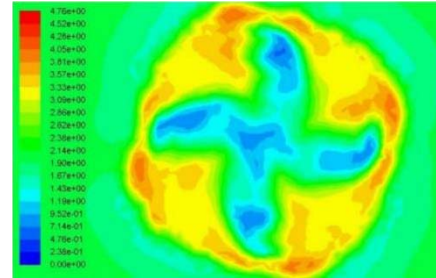


Fig. 21.1: Velocity contours in wake, 0.5 cm behind the propeller

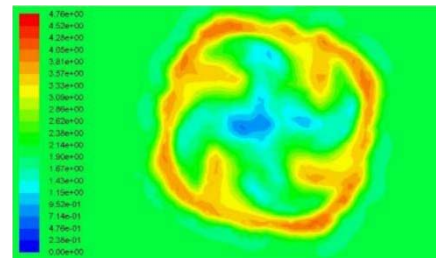


Fig. 21.2: Velocity contours in wake, 3 cm behind the propeller

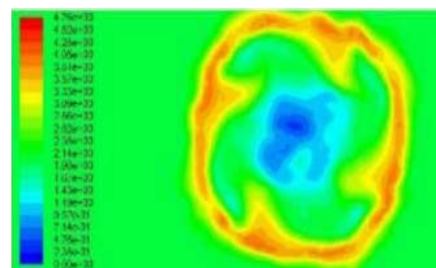


Fig. 21.3: Velocity contours in wake, 6 cm behind the propeller

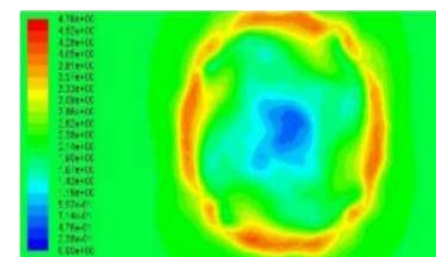


Fig. 21.4: Velocity contours in wake, 9 cm behind the propeller

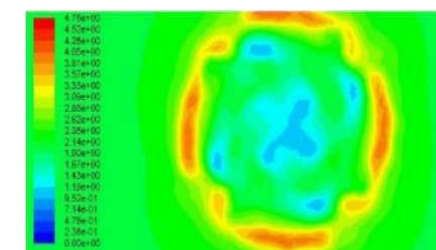


Fig. 21.5: Velocity contours in wake, 12 cm behind the propeller

Another powerful tool to understand the system is to see how the water particles traverse once they leave the propeller and advance in the wake. For this, path lines were plotted, shown in fig. 22. It shows that water particles are rotated by the propellers and the rotation of water as they advance in the wake with respect to time.

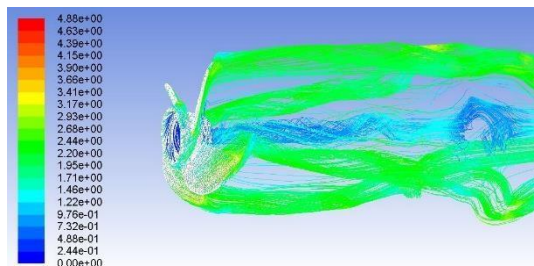


Fig. 22: Path Lines of Water Leaving Propeller

VIII.CONCLUSION

This study was meant to propose a CFD based three-dimensional design of an underwater vehicle. Solid modeling was carried out for producing the geometries of the hull and the propellers. The hulls of various shapes required to be studied were made using SolidWorks. CFD analysis on all the shapes was performed, and it was observed that drag was reduced. First, 2D CFD was carried out, and then its results were used to make an optimized 3D hull. In case of propeller, thrust was maximized. All the CFD results were also validated from the available literature. Visualization techniques in CFD are invaluable in having an insight into the system. These techniques like velocity contours and path lines were utilized to understand the behavior of system. This complete study encompassed a range of optimized parameters for designing an underwater vehicle.

ACKNOWLEDGEMENT

The authors are thankful to the Centre of Excellence in Science and Applied Technology (CESAT), Islamabad, Pakistan for funding this work. In addition, the support from the staff at the Supercomputing lab, NUST Research Center for Modeling & Simulation is highly appreciated. The authors would like to thank Mr. Abdullah Iqbal for constructive criticism of the manuscript.

REFERENCES

- [1] https://en.wikipedia.org/wiki/Autonomous_underwater_vehicle#History, visited on 12 Dec, 2016.
- [2] Arash Nemati Hayati, Seyed Mohammad Hashemi, Mehrzad Shams, "A study on the behind-hull performance of marine propellers astern autonomous underwater vehicles at diverse angles of attack". Ocean Engineering 59 (2013) 152–163, 2013.

- [3] Xiaoxu Du, Huan Wang, "ANALYSIS OF HYDRODYNAMIC CHARACTERISTICS IN THE PROCESS OF AUTONOMOUS UNDERWATER VEHICLE DOCKING". Proceedings of the ASME 2015 34th International Conference on Ocean, Offshore and Arctic Engineering OMAE2015 May 31-June 5, 2015, St. John's, Newfoundland, Canada, 2015.
- [4] George Papadopoulos, "HYDRODYNAMIC PERFORMANCE AND SHAPE CONSIDERATIONS OF A COMPACT AUV FOR RIVERINE ENVIRONMENTS". Proceedings of the ASME-JSME-KSME 2015 Joint Fluids Engineering Conference AJKFluids2015 July 26-31, 2015, Seoul, Korea
- [5] Serge Toxopeus, Roderik Kuin, Maarten Kerkvliet, "IMPROVEMENT OF RESISTANCE AND WAKE FIELD OF AN UNDERWATER VEHICLE BY OPTIMISING THE FIN-BODY JUNCTION FLOW WITH CFD". Proceedings of the ASME 2014 33rd International Conference on Ocean, Offshore and Arctic Engineering OMAE2014 June 8-13, 2014, San Francisco, California, USA.
- [6] ANSYS Fluent v14.0, ANSYS Inc., USA.
- [7] João Victor Nunes de Sousa, Antônio Roberto Lins de Macêdo, Wanderley Ferreira de Amorim Junior, Antonio Gilson Barbosa de Lima, "Numerical Analysis of Turbulent Fluid Flow and Drag Coefficient for Optimizing the AUV Hull Design". Open Journal of Fluid Dynamics, 2014, 4, 263-27, 2014.
- [8] Dongyan Zhang, "Numerical Simulation of the Hydrodynamic Performance of an Oar Blade of Canoe". 2011 International Conference on Future Computer Science and Education, 2011.
- [9] Xiao Wang, Keith Walters, "Computational Analysis of Marine-Propeller Performance Using Transition-Sensitive Turbulence Modeling". Journal of Fluids Engineering, July, 2012, Vol. 134, 2012.